# Strehl ratios characterizing optical elements designed for presbyopia compensation

**K. Petelczyc,[1,*] J. Ares García,[2] S. Bará,[3] Z. Jaroszewicz,[4,5] K. Kakarenko,[1] A. Kolodziejczyk,[1] and M. Sypek[1]**

*[1]Faculty of Physics, Warsaw University of Technology, Koszykowa 75, 00-662 Warsaw, Poland*
*[2]Departamento de Fisica Aplicada, Facultad de Ciencias, Universidad de Zaragoza, 50009 Zaragoza, Spain*
*[3]Area de Optica, E.U., Optica e Optometria, Universidade de Santiago de Compostela, 15782 Santiago de Compostela, GALIZA Spain*
*[4]Institute of Applied Optics, Kamionkowska 18, 03-805 Warsaw, Poland*
*[5]National Institute of Telecommunications, Szachowa 1, 04-894 Warsaw, Poland*
**krzys137@if.pw.edu.pl*

**Abstract:** We present results of numerical analysis of the Strehl ratio characteristics for the light sword optical element (LSOE). For comparison there were analyzed other optical imaging elements proposed for compensation of presbyopia such as the bifocal lens, the trifocal lens, the stenopeic contact lens, and elements with extended depth of focus (EDOF), such as the logarithmic and quartic axicons. The simulations were based on a human eye's model being a simplified version of the Gullstrand model. The results obtained allow to state that the LSOE exhibits much more uniform characteristics of the Strehl ratio comparing with other known hitherto elements and therefore it could be a promising aid to compensate for the insufficient accommodation range of the human eye.



**OCIS codes:** (080.2740) Geometric optical design; (110.2990) Image formation theory; (110.6890) Three-dimensional image processing; (220.3620) Lens system design; (330.4060) Vision modelling; (330.7323) Visual optics, aging changes.

## References and links

1. P. Artal, and J. Tabernero, "Optics of human eye: 400 years of exploration from Galileo's time," Appl. Opt. **49**(16), D123–D130 (2010).
2. B. K. Pierscionek, "What we know and understand about presbyopia," Clin. Exp. Optom. **76**(3), 83–90 (1993).
3. A. Glasser, M. A. Croft, and P. L. Kaufman, "Aging of the human crystalline lens and presbyopia," Int. Ophthalmol. Clin. **41**(2), 1–15 (2001).
4. A. W. Lohmann, and D. P. Paris, "Variable Fresnel zone pattern," Appl. Opt. **6**(9), 1567–1570 (1967).
5. A. Kolodziejczyk, and Z. Jaroszewicz, "Diffractive elements of variable optical power and high diffraction efficiency," Appl. Opt. **32**(23), 4317–4322 (1993).
6. A. N. Simonov, G. Vdovin, and M. C. Rombach, "Cubic optical elements for an accommodative intraocular lens," Opt. Express **14**(17), 7757–7775 (2006).
7. A. N. Simonov, G. Vdovin, and M. Loktev, "Liquid-crystal intraocular adaptive lens with wireless control," Opt. Express **15**(12), 7468–7478 (2007).
8. G. Li, D. L. Mathine, P. Valley, P. Äyräs, J. N. Haddock, M. S. Giridhar, G. Williby, J. Schwiegerling, G. R. Meredith, B. Kippelen, S. Honkanen, and N. Peyghambarian, "Switchable electro-optic diffractive lens with high efficiency for ophthalmic applications," Proc. Natl. Acad. Sci. U.S.A. **103**(16), 6100–6104 (2006).
9. G. Li, P. Valley, P. Äyräs, D. L. Mathine, S. Honkanen, and N. Peyghambarian, "High-efficiency switchable flat diffractive ophthalmic lens with three-layer electrode pattern and two-layer via structures," Appl. Phys. Lett. **90**(11), 111105 (2007).
10. R. Menapace, O. Findl, K. Kriechbaum, and Ch. Leydolt-Koeppl, "Accommodating intraocular lenses: a critical review of present and future concepts," Graefes Arch. Clin. Exp. Ophthalmol. **245**(4), 473–489 (2007).
11. W. Zhang, K. Aljasem, H. Zappe, and A. Seifert, "Completely integrated, thermo-pneumatically tunable microlens," Opt. Express **19**(3), 2347–2362 (2011).
12. W. Qiao, D. Johnson, F. S. Tsai, S. H. Cho, and Y.-H. Lo, "Bio-inspired accommodating fluidic intraocular lens," Opt. Lett. **34**(20), 3214–3216 (2009).
13. H. Lesiewska-Junk, and J. Kałuzny, "Intraocular lens movement and accommodation in eyes of young patients," J. Cataract Refract. Surg. **26**(4), 562–565 (2000).
14. O. Findl, B. Kiss, V. Petternel, R. Menapace, M. Georgopoulos, G. Rainer, and W. Drexler, "Intraocular lens movement caused by ciliary muscle contraction," J. Cataract Refract. Surg. **29**(4), 669–676 (2003).

#142708 - $15.00 USD Received 16 Feb 2011; revised 11 Mar 2011; accepted 4 Apr 2011; published 19 Apr 2011

15. J. A. Davison, and M. J. Simpson, "History and development of the apodized diffractive intraocular lens," J. Cataract Refract. Surg. **32**(5), 849–858 (2006).
16. B. Żelichowska, M. Rękas, A. Stankiewicz, A. Cerviño, and R. Montés-Micó, "Apodized diffractive versus refractive multifocal intraocular lenses: optical and visual evaluation," J. Cataract Refract. Surg. **34**(12), 2036–2042 (2008).
17. P. J. Valle, J. E. Oti, V. F. Canales, and M. P. Cagigal, "Visual axial PSF of diffractive trifocal lenses," Opt. Express **13**(7), 2782–2792 (2005).
18. J. Sochacki, A. Kołodziejczyk, Z. Jaroszewicz, and S. Bara, "Nonparaxial design of generalized axicons," Appl. Opt. **31**(25), 5326–5330 (1992).
19. W. Chi, and N. George, "Electronic imaging using a logarithmic asphere," Opt. Lett. **26**(12), 875–877 (2001).
20. J. Ares, R. Flores, S. Bara, and Z. Jaroszewicz, "Presbyopia compensation with a quartic axicon," Optom. Vis. Sci. **82**(12), 1071–1078 (2005).
21. E. R. Dowski, Jr., and W. T. Cathey, "Extended depth of field through wave-front coding," Appl. Opt. **34**(11), 1859–1866 (1995).
22. A. Kolodziejczyk, S. Bara, Z. Jaroszewicz, and M. Sypek, "The light sword optical element – a new diffraction structure with extended depth of focus," J. Mod. Opt. **37**(8), 1283–1286 (1990).
23. G. Mikuła, Z. Jaroszewicz, A. Kolodziejczyk, K. Petelczyc, and M. Sypek, "Imaging with extended focal depth by means of lenses with radial and angular modulation," Opt. Express **15**(15), 9184–9193 (2007).
24. J. Ares García, S. Bará, M. Gomez García, Z. Jaroszewicz, A. Kolodziejczyk, and K. Petelczyc, "Imaging with extended focal depth by means of the refractive light sword optical element," Opt. Express **16**(22), 18371–18378 (2008).
25. K. Petelczyc, J. Ares Garcia, S. Bará, Z. Jaroszewicz, A. Kolodziejczyk, and M. Sypek, "Presbyopia compensation with a light sword optical element of a variable diameter," Phot. Lett. Poland **1**, 55–57 (2009).
26. A. Valberg, *Light Vision Color* (John Wiley & Sons, 2005).
27. H. Gross, F. Blechinger, and B. Achtner, *Handbook of Optical Systems, Vol. 4, Survey of Optical Instruments* (Wiley-VCH, 2008).
28. M. Sypek, "Light propagation in the Fresnel region. New numerical approach," Opt. Commun. **116**(1-3), 43–48 (1995).
29. M. Sypek, C. Prokopowicz, and M. Gorecki, "Image multiplying and high-frequency oscillations effects in the Fresnel region light propagation simulation," Opt. Eng. **42**(11), 3158–3164 (2003).
30. S. Wittenberg, "Pinhole eyewear systems: a special report," J. Am. Optom. Assoc. **64**(2), 112–116 (1993).
31. J. L. Breger, "Pinhole presbyopic contact lenses," US Patent 6,283,595 (April 04 2001).
32. J. T. De Carle, "Bifocal contact lenses," US Patent 4,704,016 (March 11 1987).
33. J. H. Roffman, T. R. Poling, and M. Guillon, "Pupil-tuned multifocal ophthalmic lens," US Patent 5,448,312 (May 09 1995).
34. V. Mahajan, *Aberration theory made simple*, (SPIE Press, 1991).
35. B. W. Wang, and K. J. Ciuffreda, "Depth-of-focus of the human eye: theory and clinical implications," Surv. Ophthalmol. **51**(1), 75–85 (2006).
36. D. R. Williams, G. Y. Yoon, A. Guirao, H. Hofer, and J. Porter, "How far can we extend the limits of human vision," in *Customized corneal ablation: the quest for super vision*, S.M. MacRae, R.R. Krueger, and R.A. Applegate, eds. (Slack, 2001), pp.11–32.
37. P. Artal, "Aging effects on the optics of the eye," in *Age-Related Changes of the Human Eye (Aging Medicine)*, C.A.P. Cavallotti and L. Cerulli, eds. (Humana Press Inc., 2008), pp.35–44.

## 1. Introduction

Questions related with the human eye were and probably will remain one of the most important topics constituting the science of optics [1]. One of the most serious drawbacks of our sense of vision is the almost constant decline of the accommodation range, which decreases from a value well above 10 D at the birth till 1D or less approximately in the age of 45 ÷ 50 [2], [3]. Two principal sets of proposals to solve this problem can be recalled in this aspect. One of them, which can be termed as accommodating lenses, represent varifocal elements based on Alvarez lenses [4–6] or programmable lenses based on spatial light modulators (SLMs) [7–9]. There were proposed also tunable lenses acting similarly to the eye's crystalline lens [10–12] or solutions where the change of the optical power takes place due to the axial displacement of a fixed-focus lens [13], [14]. The second group is formed by the static elements, which can be sub-divided further into multifocal refractive or diffractive intraocular lenses (IOLs) [15–17], forming a set of few foci (usually two or three) or the EDOF elements. In the last group we find axicons [18–20], cubic masks [21] and LSOE [22]. This last element was found recently as an interesting option because of its relatively good image quality [23], [24], which remains almost independent on the pupil's diameter [25].

The present paper deals with a comparison of the imaging properties of the most popular elements designed for presbyopia compensation with the LSOE. For this purpose the Strehl

#142708 - $15.00 USD Received 16 Feb 2011; revised 11 Mar 2011; accepted 4 Apr 2011; published 19 Apr 2011

ratio was chosen. The comparison was performed using the Gullstrand model of the human eye [26], [27], which was modified according to the specific needs of our problem and software package for simulation of the light diffraction [28], [29].

## 2. Eye model

The schematic eye model, which will be used for simulations, on one hand must be sufficiently simple, whereas on the other one it should offer adequate simulation's accuracy. Our starting point was the Gullstrand eye model without accomodation [26], [27].

In our analysis we limit our attention to the foveal region. It allows to relieve the computational effort of the simulation and to use the paraxial approximation for the optical elements composing the model. Our assumption is justified because this retina's area allows to obtain vision of highest resolution and quality.

Our approximation allows also to simplify the presbyopic eye's model to the set-up shown in Fig. 1, where the cornea is represented by a lens of 43 D placed 5.38 mm in front of the second lens substituting a presbyopic eye with optical power equal to 19.2 D. The distance between the retinal plane and the second lens is assumed to be 18.76 mm. The refraction index value of the liquid between the cornea, the lens and the retina is taken as 1.336. The pupil and the contact lens representing the optical element compensating presbyopia are placed in front of the first lens substituting the cornea.

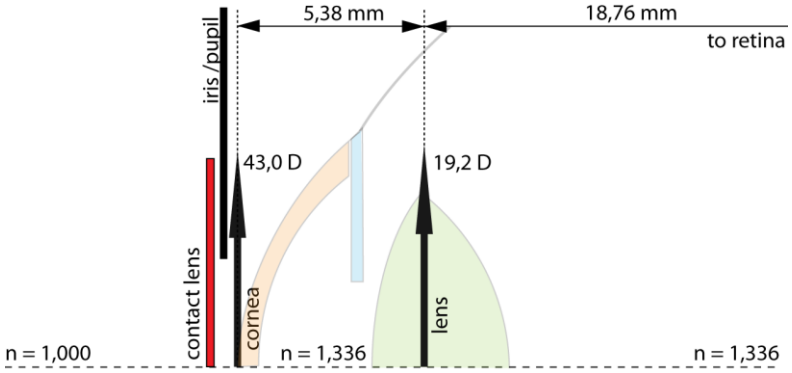


Fig. 1. Eye model assumed in the modeling and its parameters. Gullstrand unaccommodated eye geometry in a background.

## 3. Presbyopia compensating elements

As the first element and a reference for the next ones, marked as EYE, we take the presbyopic naked eye without any aid. It gives sharp images, when the object plane is placed at infinity. The next element (RG) is EYE together with reading glasses of 4D designed for an object plane located at the distance of 25 cm. Then follow: PCL – EYE with stenopeic pinhole contact lens limiting the aperture [30], [31] and representing the simplest solution for increasing the depth of focus, ASCL – EYE with bifocal angular sectors contact lens [32], BFCL – EYE with annularly oriented bifocal contact lens [33] used in Acuvue Bifocal® contact lenses, MFCL – EYE with annularly oriented multifocal contact lens used in CL Lifestyle X-tra contact lenses (The Lifestyle Company Inc., Morganville, NJ), ILAX – EYE with inverse logarithmic axicon [18] and IQAX – EYE with inverse quartic axicon [20]. Both axicons can be regarded as spherical lenses with a specially designed addition of spherical aberration and the quartic one as an approximation of the logarithmic axicon. The next to last element is LSOE – EYE with conventional LSOE [22–25]. The distribution of the optical path difference due to the LSOE is given by:

#142708 - $15.00 USD Received 16 Feb 2011; revised 11 Mar 2011; accepted 4 Apr 2011; published 19 Apr 2011

$$\Delta l(r,\quad \theta) = \frac{r^2}{2\left[ f_1 + (\Delta f\,\theta / 2\pi)\right]}, \tag{1}$$

where $r$, $\theta$ are the radial and azimuthal coordinates respectively and parameters $f_1$ and $\Delta f$ stand for the focal length and the focal range of the element. For a fixed value of the angular argument $\theta$ the optical path difference is equivalent to that of a spherical lens with a focal length $f_1 + \Delta f\,\theta\,/2\pi$. Therefore in a first approximation the LSOE focuses an incident plane wave into a focal segment of a width $\Delta f$. The last element aLSOE is characterized by dioptric power varying linearly in function of an angle and represents a different solution from the previous one, a LSOE with linearly variable focal length:

$$\Delta l(r,\quad \theta) = Cr^2 + D\theta r^2, \text{where } C = 1/2\,f_1 \quad D = \frac{1}{4\pi}\left(\frac{1}{f_1} - \frac{1}{f_1 + \Delta f}\right), \tag{2}$$

The shape of the LSOE and aLSOE elements together with their focusing geometry is shown in Fig. 2. Every infinitesimal sector of these elements is supposed to focus light into the corresponding point situated within the focal segment. However, focusing is approximate only and in reality instead of point focus we observe a small focal segment perpendicular to the optical axis [24].

Distributions of dioptric powers of all elements compared in this work are shown in Fig. 3.

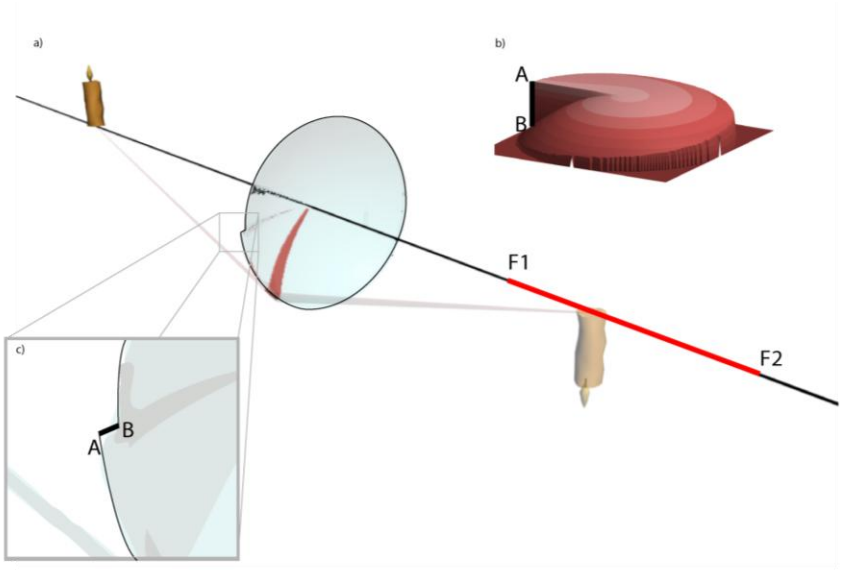


Fig. 2. Shape of the LSOE and aLSOE elements and their scheme of imaging. The infinitesimal angular sector of the element images object from different distance (a). Element has a sharp step in geometrical profile (b) equal to shape's maximum difference between 0D and 4D lens(c).

#142708 - $15.00 USD Received 16 Feb 2011; revised 11 Mar 2011; accepted 4 Apr 2011; published 19 Apr 2011

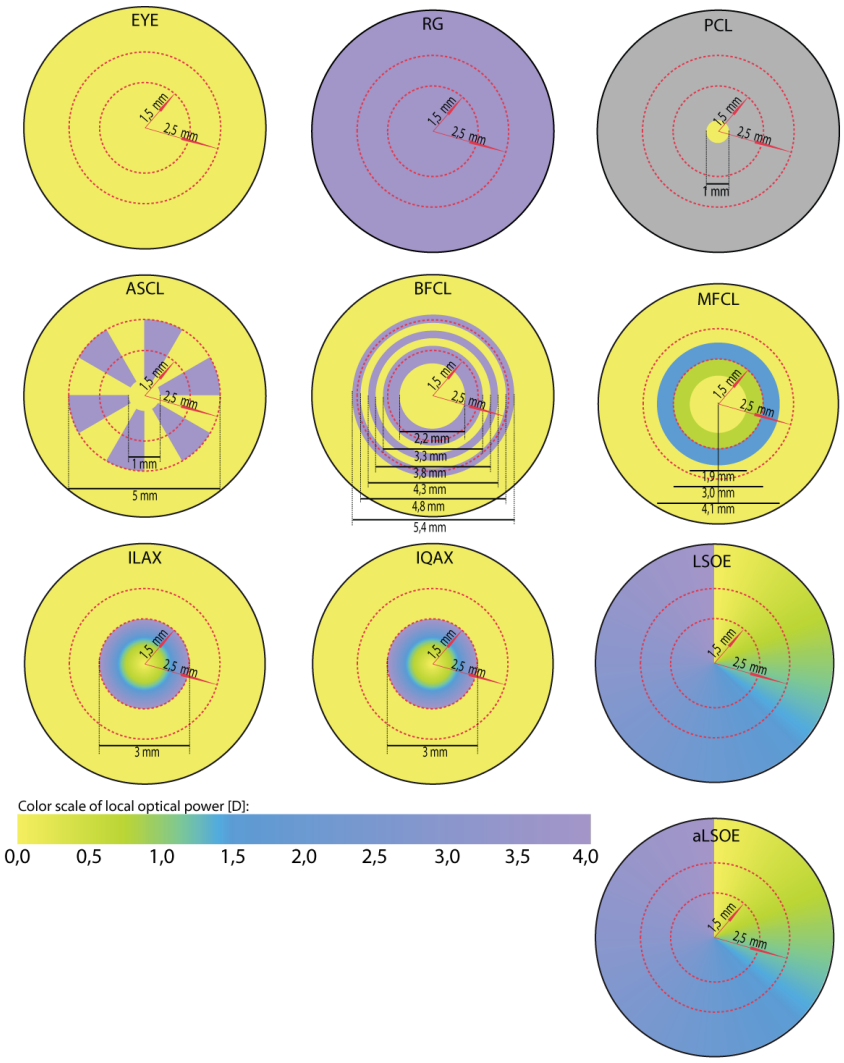


Fig. 3. Optical elements used in simulation. Their diameter was assumed to be equal to 8 mm. The used abbreviations were explained in the text. The optical power corresponding to different areas is marked with the color bar.

## 3. Results of simulation

In order to compare the performance of the elements intended for presbyopia compensation, the Strehl ratio was chosen. It can range from 0 to 1 and is defined as the ratio of the peak intensity of the eye's PSF $I_{Max,\ \Phi}$ to that of a diffraction limited PSF $I_{Max,\ \Phi=0}$ for an aberration-free eye (i.e., for $\Phi = 0$) with the same pupil size [34]:

$$S = I_{Max,\ \Phi} / I_{Max,\ \Phi=0} \tag{3}$$

Distributions of the Strehl ratios for all optical elements listed in the previous chapter are shown in Fig. 4. In our simulations we limit the apertures' diameter up to 5 mm. This value usually corresponds to the maximum eye pupil in normal photopic vision.

#142708 - $15.00 USD Received 16 Feb 2011; revised 11 Mar 2011; accepted 4 Apr 2011; published 19 Apr 2011

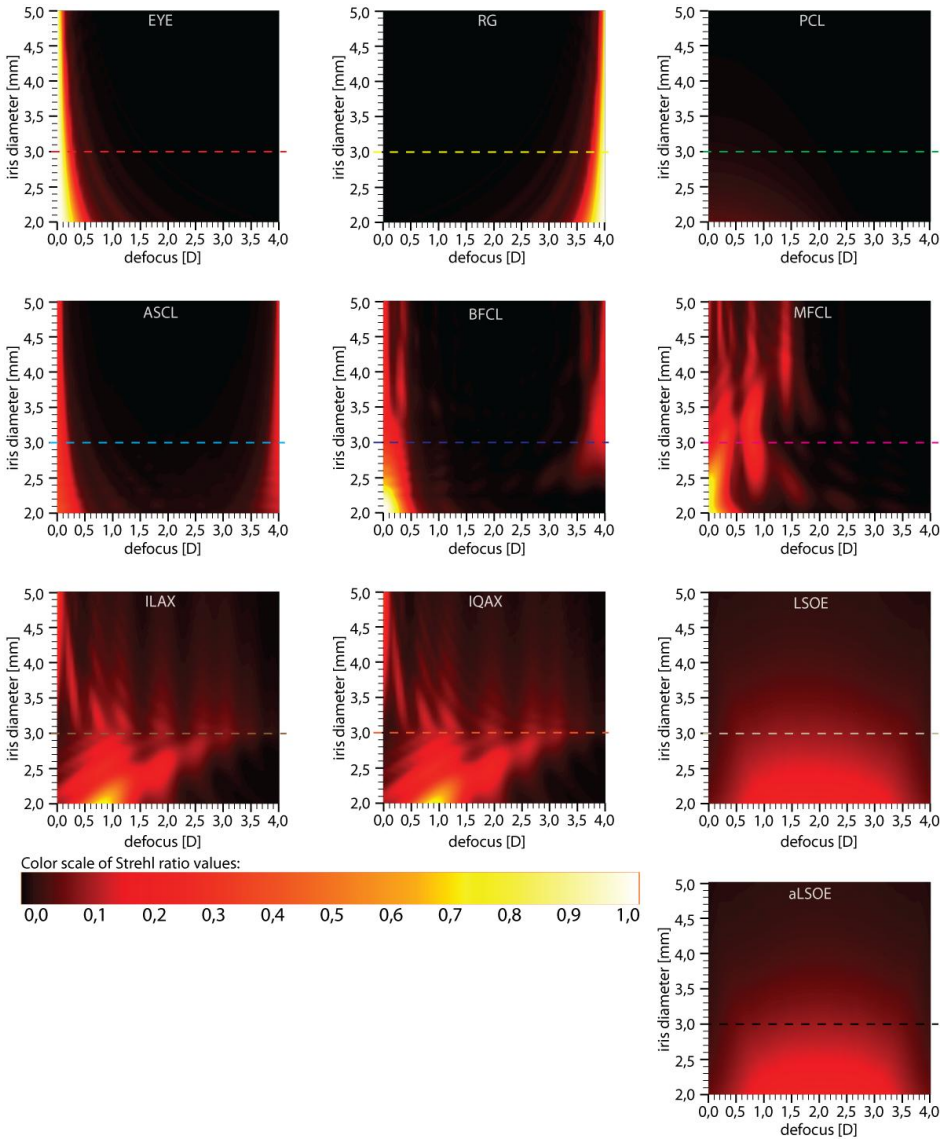


Fig. 4. Strehl ratios for different values of elements diameter and for different values of defocus.

The results were obtained by using the numerical software for diffraction simulation [28], [29] with use of monochromatic light of wavelenghth 555 nm coresponding to maximum sensitivity of photopic vision [26]. Images of the point sources placed at distances corresponding to values of defocus from 0 till 4 D were calculated at the retinal plane after passing the compensating element and two lenses located as it was shown in Fig. 1. The whole procedure of Strehl ratio determination was as follows: generation of diverging spherical wave corresponding to the defocus value of the plot, multiplication by the transmittance of the element correcting the presbyopia, multiplication by the transmittance of cornea and an amplitude distribution equal to $\exp(-0.053r^2)$ corresponding to the Stiles-Crawford effect, propagation by a distance of 5,4 mm in a medium with refraction index equal to 1,336, multiplication by the transmittance of the eye lens, and propagation to the retina by a distance of 18,76 mm. Then the Strehl ratio was obtained by finding the maximum value of

#142708 - $15.00 USD Received 16 Feb 2011; revised 11 Mar 2011; accepted 4 Apr 2011; published 19 Apr 2011

the PSF obtained in the above way and its division by the analogous value for PSF obtained without correcting element and with zero defocus.

Looking on the results shown in Fig. 4 one can state that the LSOE offers the best uniformity comparing with any other element, maybe except of the stenopeic lens (although in this last case the price which has to be paid is a significant loss of light resulting in the average value of the Strehl ratio in the whole range of distances as smaller than 0.015). On the other hand both axicons, as well as bifocal and multifocal lenses show small regions with superior values of the Strehl ratio, but at the price of its lack of uniformity. Usually these ranges are smaller or at most comparable with typical values of the depth of focus, which for the human eye at normal conditions of illumination is of order of 0.5 D [35]. Contrary to these elements, for the aperture diameter of 3 mm the Strehl ratio value for LSOE and aLSOE was equal approximately to 10% across the whole range of defocus. According to Eq. (2), the maximum value of the discontinuity marked as the segment AB in Fig. 1 for the assumed values of parameters is 25 μm, what should not to be very harmful.

## 4. Conclusions

We presented results of simulation for the Strehl ratio of the LSOE and its comparison with other elements proposed up to the present for presbyopia compensation, such as: the stenopeic lens, the bifocal lens, the trifocal lens, the logarithmic axicon and the quartic axicon. The obtained results show visibly the superiority of the LSOE's Strehl number characteristics over all other solutions in terms of the Strehl's ratio uniformity. It maintains almost a constant value along the whole length of the focal segment, i.e., within the whole range of accommodation aimed to be covered and assumed to be equal to 4 D, whereas the remaining proposals exhibit significant variations. According to the previous publications the diffractive LSOE can be successfully applied for imaging with extended depth of focus for monochromatic illumination [22 [23]. Recently it was demonstrated experimentally that the refractive version of LSOE has chromatic aberrations small enough as not to disturb visually imaging in white light [24], [25]. There remains to answer the problem of the observer's acceptance of the halo surrounding the PSF core. However the problem of halo seems to exert smaller influence than in the case of other EDOF elements, what probably is due to the asymmetrical PSF of the LSOE and probably is easier to compensate by the brain image processing procedures. Let us observe additionally that the value of the Strehl number within the whole accommodation range does not fall below the level of 0.3, what is comparable with commonly encountered values in the case of normal and unaided vision [36], [37]. The present results, though promising, should be considered as preliminary only and further studies are needed in order to determine the influence of the real eye aberrations onto the LSOE performance as well as its psychophysical adaptability.

## Acknowledgment

This work was supported by the Polish Ministry of Science and Higher Education under grants N N 514 149038 and N N 518 378237 as well as by the European Social Fund implemented under the Human Capital Operational Programme (POKL), project: "Preparation and Realization of Medical Physics Specialty" with complementary support from the Spanish Ministerio de Ciencia e Innovación (MICINN) grant FIS2008-03884.

#142708 - $15.00 USD Received 16 Feb 2011; revised 11 Mar 2011; accepted 4 Apr 2011; published 19 Apr 2011